Electronic Supplementary Material (ESI) for Catalysis Science & Technology.
This journal is © The Royal Society of Chemistry 2019

Supporting Information for

Catalytic activation of ethylene C-H bonds on uniform d^8 Ir(I) and Ni(II) cations in zeolites: toward molecular level understanding of ethylene polymerization on heterogeneous catalysts

Nicholas R. Jaegers[1,2,&,*], Konstantin Khivantsev[1,&,*], Libor Kovarik[1], Daniel W. Klas[1], Jian Zhi Hu[1], Yong Wang[1,2] and Janos Szanyi[1,&,*]

[1]Institute for Integrated Catalysis, Pacific Northwest National Laboratory Richland, WA 99352 USA

[2]Voiland School of Chemical Engineering and Bioengineering, Washington State University, Pullman, WA 99163 USA

*corresponding authors: Nicholas.Jaegers@pnnl.gov, Konstantin.Khivantsev@pnnl.gov, Janos.Szanyi@pnnl.gov

Experimental Methods

Faujasite and Beta zeolites with Si/Al of ~15 and 12.5 respectively, were supplied by Zeolyst in the ammonium form. Transformation of faujasite to the H-form was conducted by calcination in flowing dry air at 400ºC followed by evacuation at 10^{-5} Torr and 400ºC. It was subsequently stored in a VAC moisture- and oxygen-free glovebox. Single iridium atoms were then anchored in the micropore supercages of the prepared H-FAU zeolite. To ensure suitable dispersion, a well-defined square planar $Ir(CO)_2(Acac)$ complex (strem, >98% purity) was delivered into the micropores via a non-polar solvent propagation method[12,17,18]. More specifically, the precursor was dissolved in pentane (Sigma Aldrich, <10 ppm moisture) and introduced into the faujasite. Approximately 26 mg of the Ir complex was dissolved in ~10 ml dry pentane under intense stirring; then the solution was added through the needle into the Schlenk flask containing 2.00 grams of calcined dry H-FAU powder. $Ir(CO)_2$ fragments anchors to the zeolite through framework oxygen adjacent to Al T-atoms during this process. The pentane solution was subsequently evacuated for 5 hours under 10^{-5} Torr vacuum, leaving a dry powder of 0.7 wt% Ir/H-FAU.

Ni-BEA was synthesized by the modified IWI method we previously reported. In this, the NH_4-form of BEA with Si/Al~12.5 was used as the supporting zeolite. Nickel nitrate hexahydrate (Sigma Aldrich, 99.99%) was dissolved in a water/ammonia solution, producing a purple-coloured $[Ni(II)(NH_3)_6]$ complex with concentration 0.0757 M. The ammonia concentration was ~1.5 M. One pore volume equivalent (~0.9 cc/g BEA) of this solution was slowly introduced into zeolite powder with carefully mixing each aliquot. The resulting paste was dried at 80 ºC in flowing air and then calcined at 550ºC for 5 hours in a box furnace, yielding 0.4 wt% Ni/H-BEA.

The in situ static transmission IR experiments for Ni/BEA were conducted in a home-built cell housed in the sample compartment of a Bruker Vertex 80 spectrometer, equipped with an MCT detector and operated at 4 cm^{-1} resolution. The powder sample was pressed onto a tungsten mesh which, in turn, was mounted onto a copper heating assembly attached to a ceramic feedthrough. The sample could be resistively heated with temperature monitoring by a thermocouple spot welded onto the top center of the tungsten grid. Cold fingers on the CO-containing glass bulb were cooled with liquid nitrogen to prevent contamination by metal carbonyls. NO was cleaned with multiple freeze–pump–thaw cycles. Special-grade ethylene (OxArc) with 99.995% purity was cleaned with liquid nitrogen prior to use to remove traces of moisture. The activated sample was employed as the spectrum background. Each spectrum reported is obtained from the average of 256 scans. Experiments at 77 K were performed with liquid nitrogen used as a coolant. Prior to FTIR measurements, the sample was activated by heating under vacuum at 200ºC to remove moisture. All dosed gases were undiluted.

DRIFTS spectra for Ir/FAU were recorded on a Nicolet iS50R FTIR spectrometer at 4 cm^{-1} resolution. The Ir/FAU powder was packed into the DRIFTS cell inside the dry glovebox, sealed and transferred to the FTIR where it was immediately connected to the gas manifold and exposed to flowing dry He. Special-grade ethylene (99.995% purity, OxArc) and UHP C_2D_4 was used for all experiments and UHP He flowing through oxygen and moisture traps was used as the inert gas. Spectra were referenced to an H-FAU background and 64 scans were averaged in each spectrum. Samples were loaded in a dry N_2 glovebox and transferred under N_2 to the infrared spectrometer. First the sample was purged with helium, and then experiments with pure ethylene or hydrogen flow were performed. Flow rates were ~10 cc/min.

HAADF-STEM analysis was performed with an FEI Titan 80-300 microscope operated at 300 kV. The instrument is equipped with a CEOS GmbH double-hexapole aberration corrector for the

probe-forming lens which allows for imaging with 0.1 nm resolution in scanning transmission electron microscopy mode (STEM). The images were acquired with a high angle annular dark field (HAADF) detector with inner collection angle set to 52 mrad. The fresh Ir/FAU sample was loaded with no exposure to air. Spent Ir/FAU (220ºC under typical reaction conditions) was cooled down in the plug-flow reactor, purged with inert gas, and stored in the glove box prior to loading into HAADF-STEM without exposure to air. The images were collected in various projection, tilted slightly off the zone axis (to better visualize the Ir atoms), and imaged immediately to minimize beam damage during the experiment. EDS maps of O, Si, Al, and Ni were obtained for Ni/BEA in order to better visualize presence of low-contrast Ni (compared to high-contrast Ir).

The reaction measurements were performed in a typical plug-flow quartz reactor. Samples were loaded into the reactor in the glove box and purged with dry (Restek O_2/H_2O traps) He before reaction. Ethylene (OxArc, 99.995% purity) was delivered into the system through a separate set of moisture and oxygen traps. Approximately ~30 mg of catalyst powder was loaded into the quartz reactor for each run. The ethylene flow rate was ~10 sccm/min in the undiluted stream to achieve a residence time of ~0.2 s. An Agilent 7890 Gas Chromatograph equipped with an FID was used to analyze the system effluent. An Agilent HP-PLOT/Q column (30m, 0.53, 40 μm film) was used for separation. Hydrocarbons response factors were calibrated with hydrocarbon mixtures. Turn-over frequencies with respect to butadiene formation were calculated by the moles of butadiene produced divided by the moles of metal loaded into the zeolite sample per hour. Turn-over frequencies with respect to ethylene consumption towards butadiene formation were calculated by the moles of butadiene produced times two divided by the moles of metal loaded into the zeolite sample per hour. Turn-over frequencies with respect to butene formation were calculated by the total moles of all butenes produced divided by the moles of metal loaded into the zeolite sample per hour. Selectivities were calculated as the moles of the C4 chemical of interest formed divided by the total C4 chemicals simultaneously produced.

^{27}Al MAS NMR measurements were performed at room temperature on a Bruker 850 MHz NMR spectrometer operating at a magnetic field of 19.975 T. The corresponding ^{27}Al Larmor frequency was 221.413 MHz. All spectra were acquired at a sample spinning rate of 18.0 kHz (± 5 Hz) and externally referenced to 1.0 M aqueous $Al(NO_3)_3$ (0 ppm). ^{13}C and ^{1}H-^{13}C CP measurements were conducted on a Varian Inova 300 MHz spectrometers. The corresponding 13C Larmor frequency was 75.43 MHz. Spectra were externally referenced to adamantae at 38.48 ppm and a sample spinning rate of 3.4 kHz at the magic angle was employed.

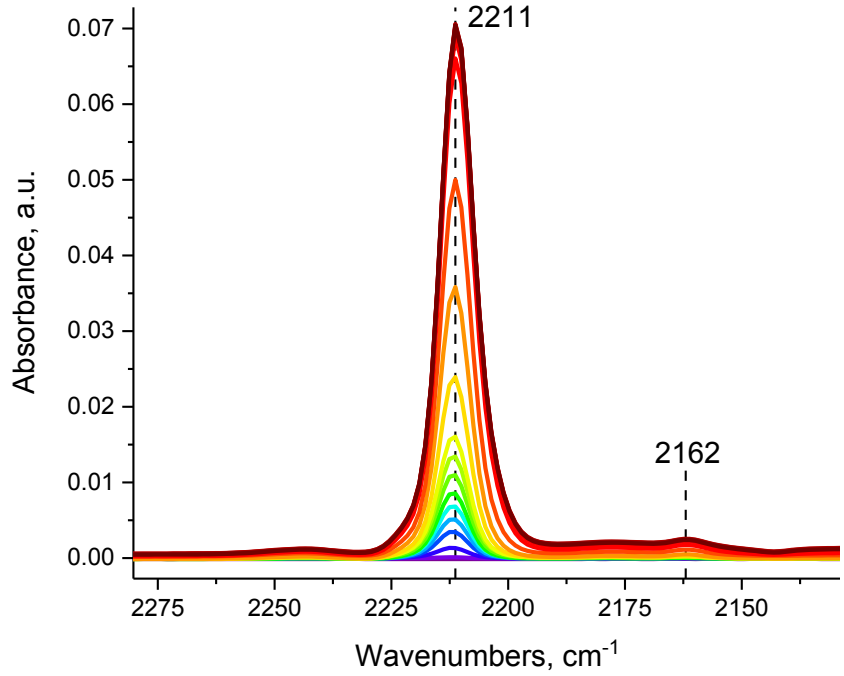

Figure S1. FTIR during CO adsorption on dry 0.4% Ni/BEA, $P(CO)_{max}$ =5 Torr.

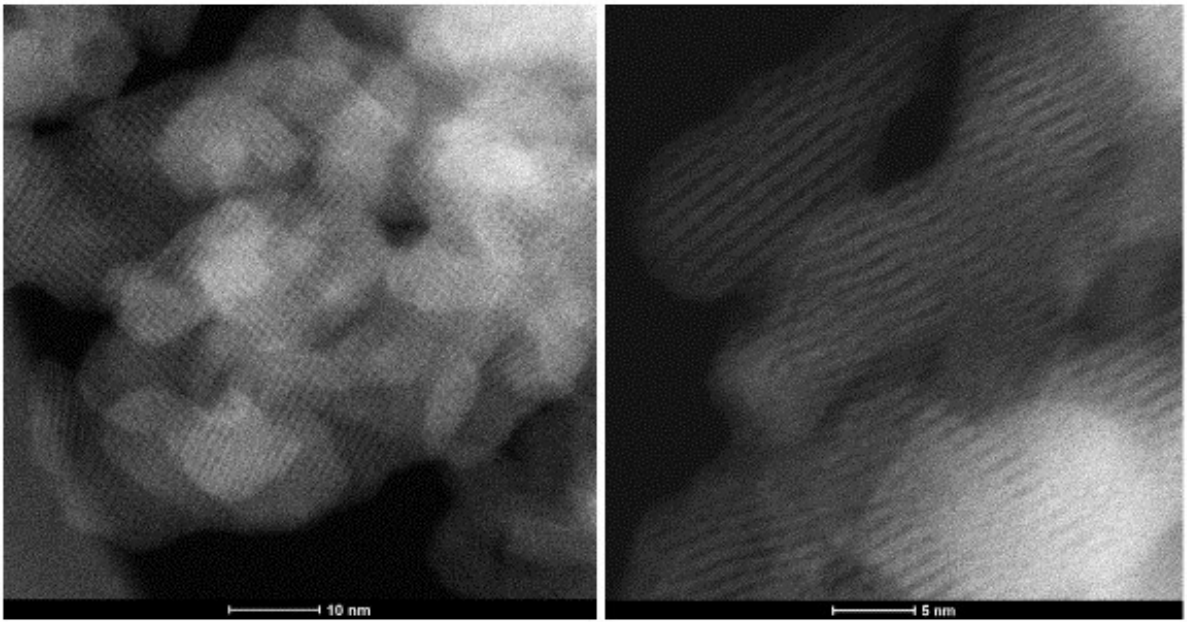

Figure S2. HAADF-STEM images of 0.4% Ni/BEA in different projections.

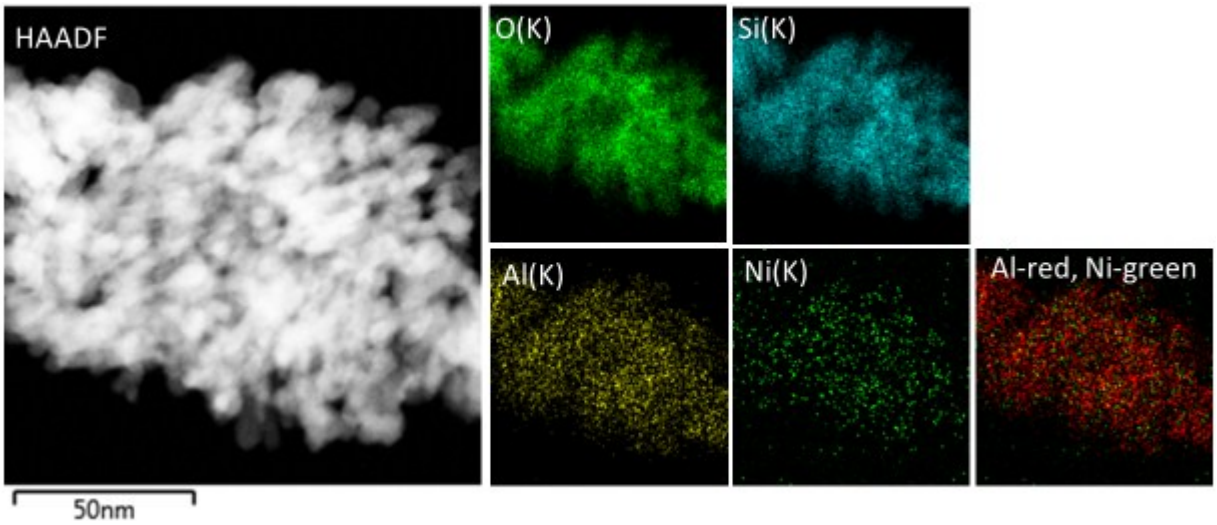

Figure S3. EDS maps of 0.4% Ni/BEA for O, Si, Al, Ni, overlay of Al and Ni maps, as well as the corresponding HAADF-STEM image for which EDS maps were collected.

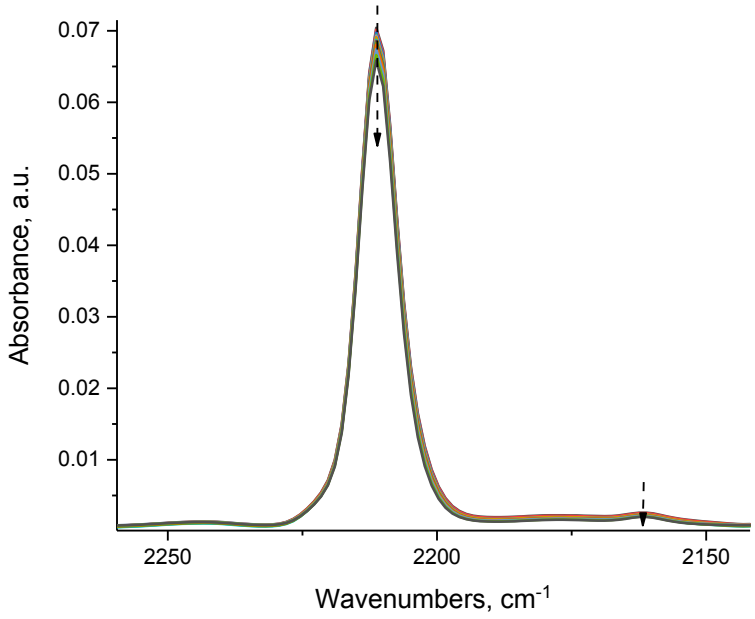

Figure S4. FTIR during vacuuming of Ni(II)-CO complex; Ni(II)-CO resists evacuation at RT. Final P=0.05 Torr.

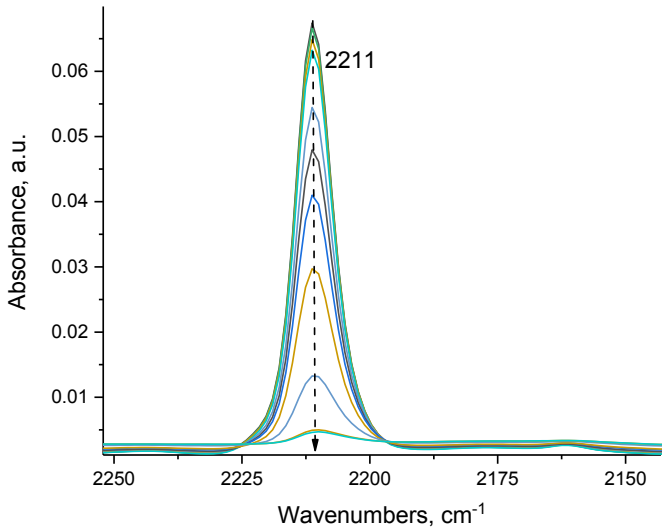

Figure S5. FTIR during ethylene adsorption (5 Torr) on Ni(II)-CO complex at RT. Ethylene completely displaces CO Ni(II)-CO + C_2H_4 → Ni-(C_2H_4) + CO

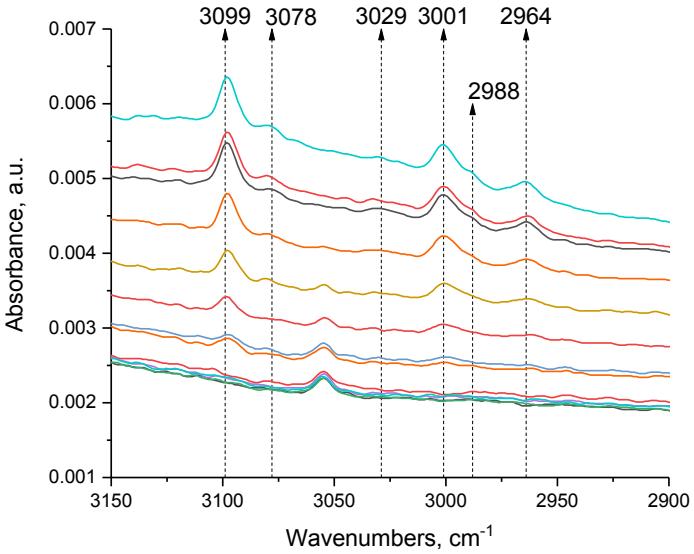

Figure S6. FTIR in the CH-stretching region during ethylene adsorption (5 Torr) on Ni(II)-CO complex at RT. The bands at 3,099, 3,078, 3,029 and 3,001 cm^{-1} are typical for pi-coordinated $H_2C{=}CH_2$ adsorbed on a d^8 metal center in organometallic compounds, such as in Rh(I) and Pd(II) in zeolite (ref 22 in the main text).

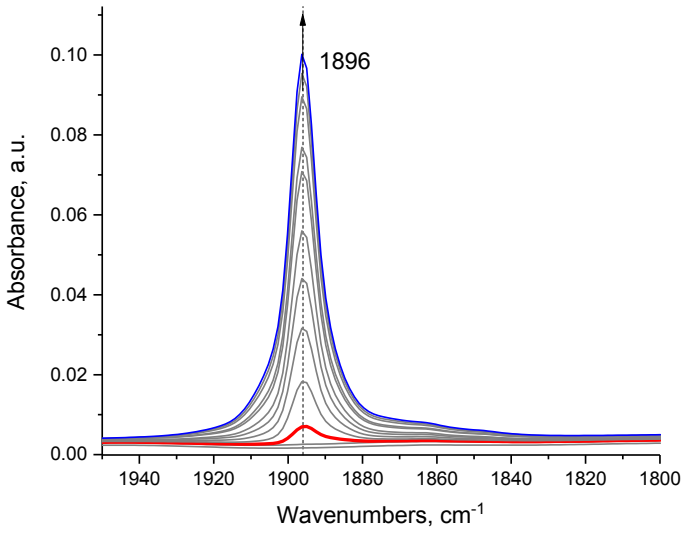

Figure S7. FTIR during NO adsorption on dry 0.4% Ni/BEA, P(NO)max=5 Torr; One type of Ni(II)-NO complex is formed. The FWHM of the NO band is ~12 cm^{-1}.

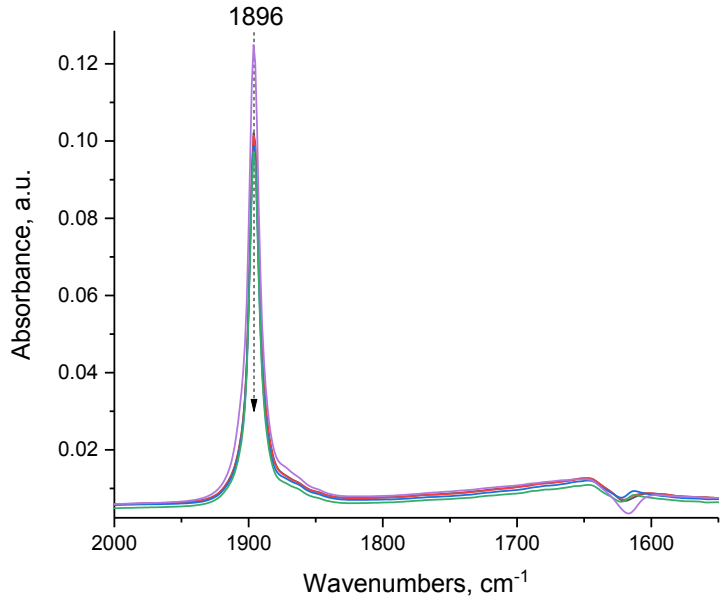

Figure S8. FTIR during vacuuming of Ni(II)-NO complex; Ni(II)-NO resists evacuation at RT. Final P=0.02 Torr.

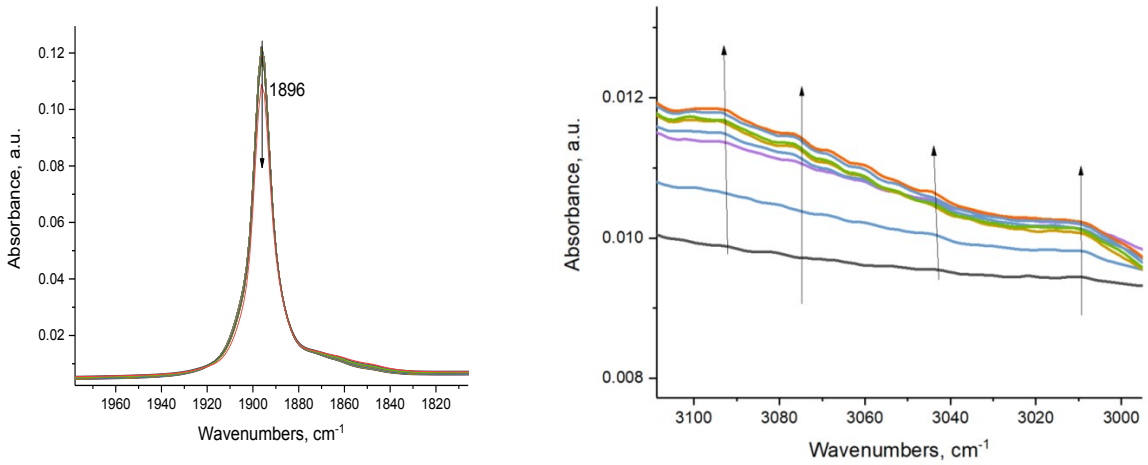

Figure S9. FTIR during ethylene adsorption (0.2 Torr) at RT on Ni(II)-NO. Ethylene displaces NO: Ni(II)-NO + C_2H_4 → Ni-(C_2H_4) + NO

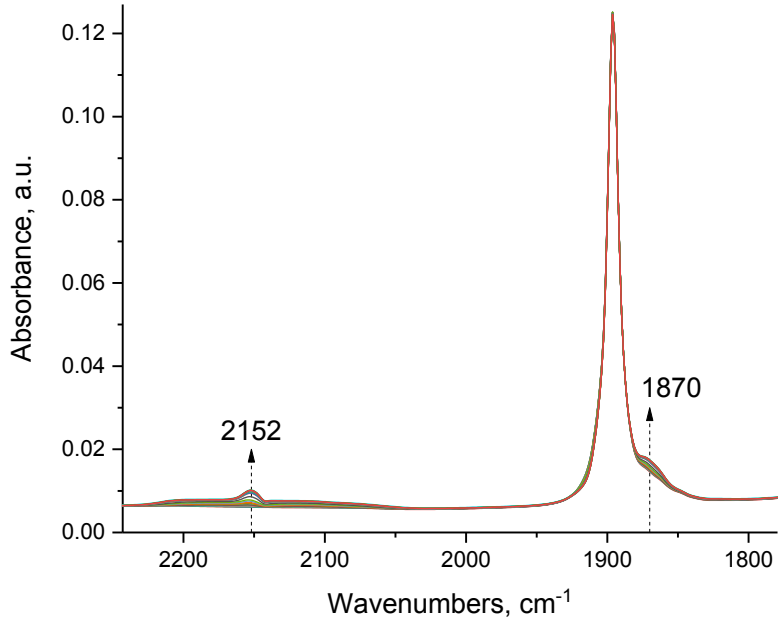

Figure S10. FTIR during CO adsorption (1 Torr) on the Ni(II)-NO complex. Ni(II)-NO is not displaced by CO, instead it forms Ni(II)(NO)(CO) complex with CO stretch at 2,152 cm^{-1} and NO stretch at 1,870 cm^{-1}.

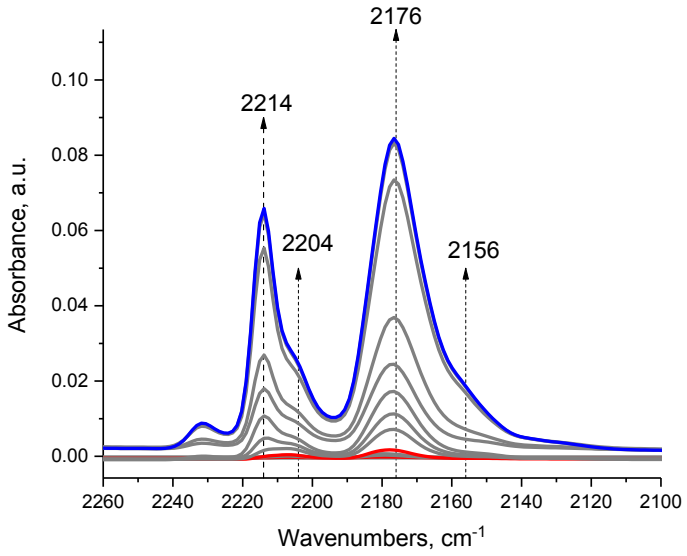

Figure S11. FTIR during CO adsorption (5 Torr) on 0.4% Ni(II)/BEA at liquid nitrogen (77 K) temperature. 2,214 and 2,204 cm^{-1} belong to CO adsorbed on Ni(II) ions. The 2,176 cm^{-1} band belong is CO adsorbed on Brönsted acid protons of H-BEA, the 2,156 cm^{-1} band is CO interacting with silanols.

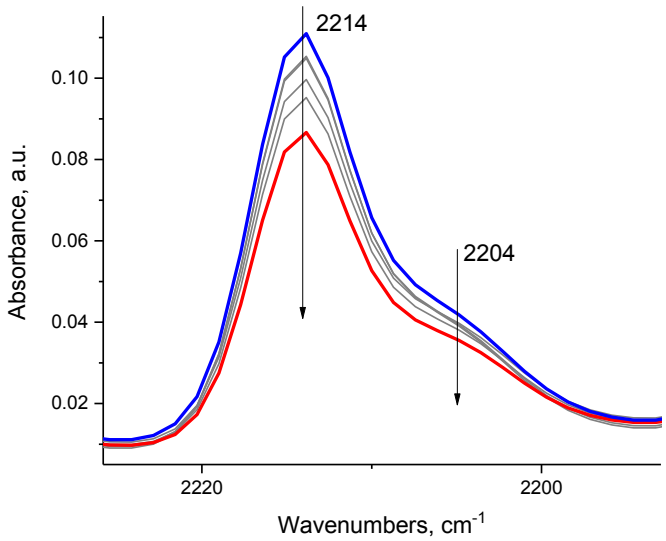

Figure S12. FTIR during vacuuming at liquid nitrogen temperature (77 K) of Ni(II)-CO complexes.

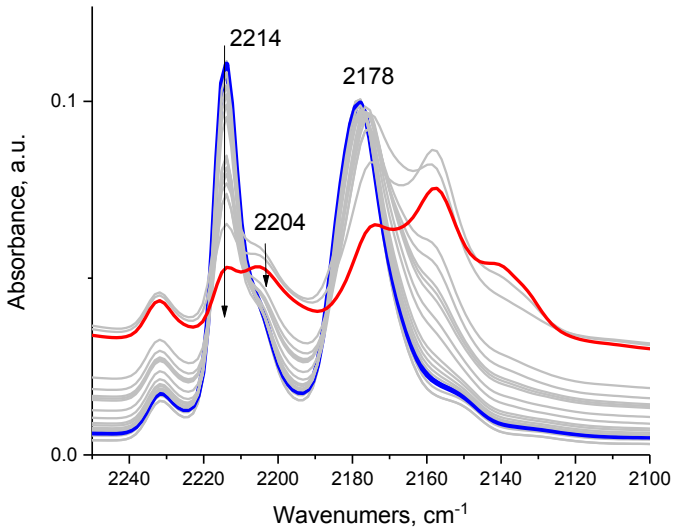

Figure S13. FTIR during C_2H_4 adsorption (2 Torr) at liquid nitrogen temperature (77 K) on Ni(II)-CO complexes. The 2,214 and 2,204 cm^{-1} CO bands of Ni(II)-CO complexes demonstrate markedly different behavior: the 2,214 cm^{-1} band decreases quickly but the 2,204 cm^{-1} band is relatively stable. This indicates that 2,214 and 2,204 cm^{-1} bands do not belong to a Ni(II)$(CO)_2$ dicarbonyl complex but to two different NI(II)-CO complexes, in which the 2,214 cm^{-1} [belonging to one Ni(II)-CO complex] is very susceptible to ligand replacement with ethylene even at 77K: Ni(II)-CO + C_2H_4 → Ni(II)-C_2H_4 + CO. Peculiarly, C_2H_4 easily displaces CO adsorbed on Brönsted acid protons of H-BEA (band at 2176 cm^{-1}).

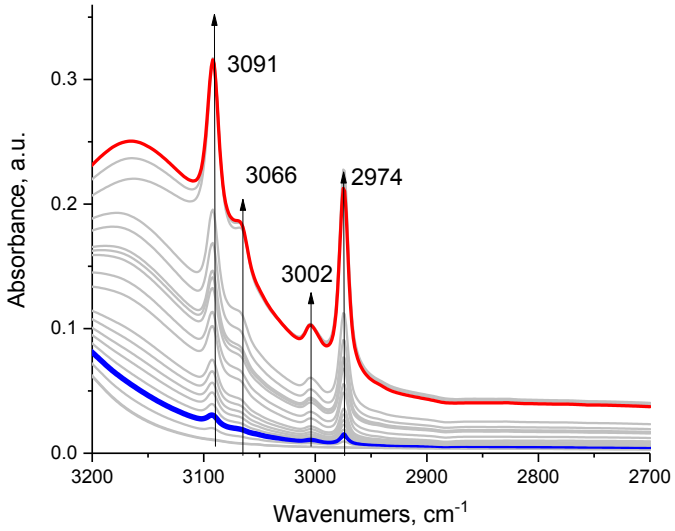

Figure S14. FTIR in the CH-stretching region during C_2H_4 adsorption (2 Torr) at liquid nitrogen temperature (77 K) on Ni(II)-CO complexes that were formed at 77 K (complimentary to Figure S13). The unusually intense bands at 3,091-2,074 cm^{-1} correspond to pi-coordinated $H_2C{=}CH_2$ interacting with –OH groups of zeolite: although this interaction is much weaker at RT, at liquid nitrogen such complexes are significantly more stable, thus the high intensity of these bands.

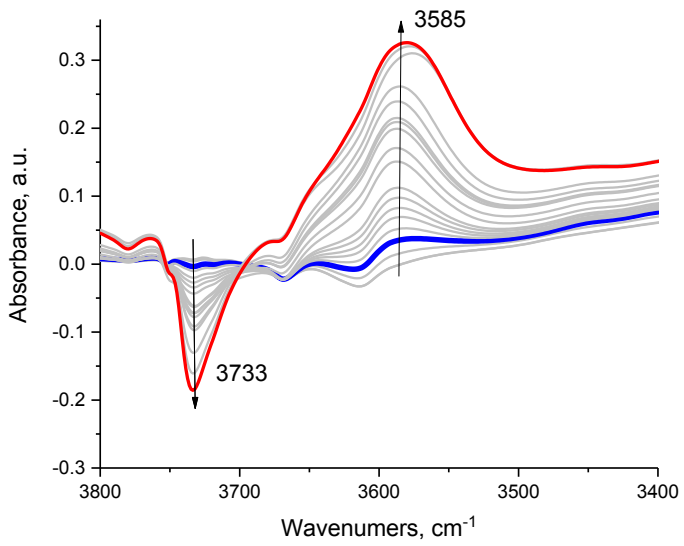

Figure S15. FTIR in the OH-stretching region during C_2H_4 adsorption (2 Torr) at liquid nitrogen temperature (77 K) on Ni(II)-CO complexes that were formed at 77 K (complimentary to Figure S13). OH bands of silanols at ~3,730 cm^{-1} decreases and forms a broad band at ~3,580 cm-1 due to formation of –OH--Ethylene adducts.

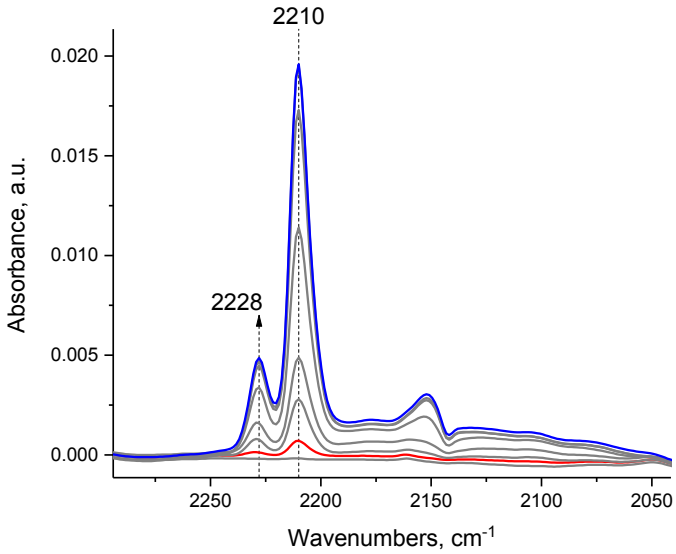

Figure S16. FTIR during CO adsorption (5 Torr) at RT on 0.4% Ni/BEA after C_2H_4 catalysis for 1 hr at 200ºC in the FTIR cell.

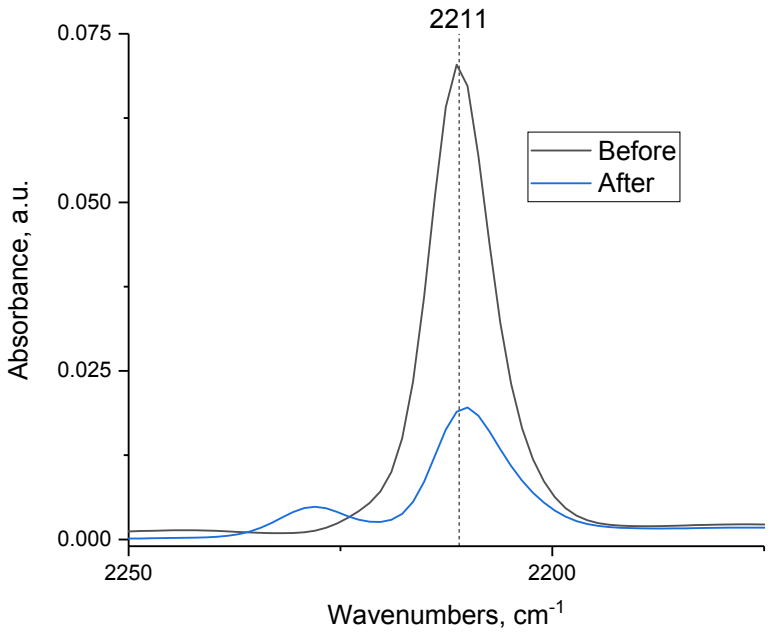

Figure S17. FTIR during adsorption of CO on dry 0.4% Ni/BEA P(CO)max=5 Torr, before and after exposed to C_2H_4 at 200ºC in the FTIR cell for 1 hr; Only one type of Ni(II)-CO complex forms. The ~2,228 cm^{-1} CO band is ascribed to CO adsorbed on extra-framework Al(III) sites. The FWHM of the CO band is ~ 9-10 cm^{-1}.

Table S1. Initial TOF (with respect to butadiene formation) and selectivity to butadiene for 0.4% Ni/BEA. Conditions: 30 mg, C_2H_4 flow rate 10 sccm/min, GHSV ~ 40,000 hr^{-1}

Temperature, ºC	Initial TOF, hr^{-1}	Initial Selectivity, %
80	6.7	35
120	122	65
200	203	29
250	180	31

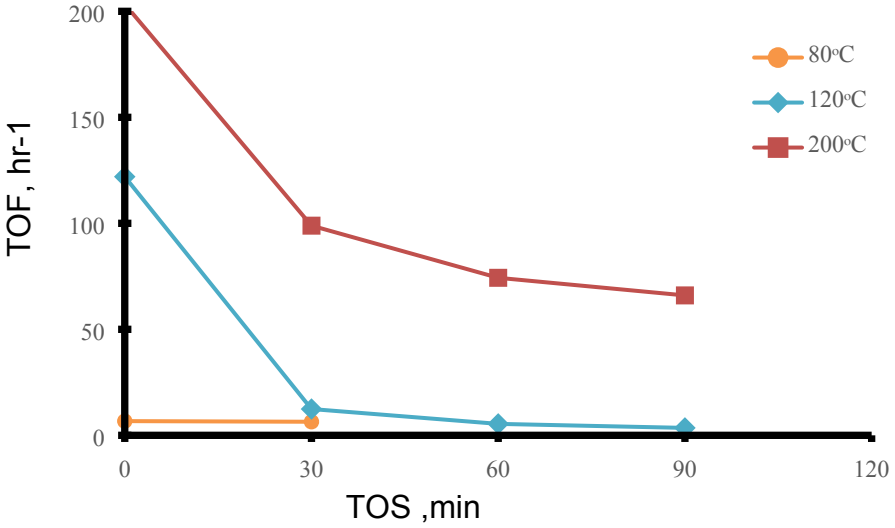

Figure S18. TOF (with respect to butadiene formation) trends as a function of time on stream for 0.4% Ni/BEA. Conditions: 30 mg, C_2H_4 flow rate 10 sccm/min, GHSV ~ 40,000 hr^{-1}

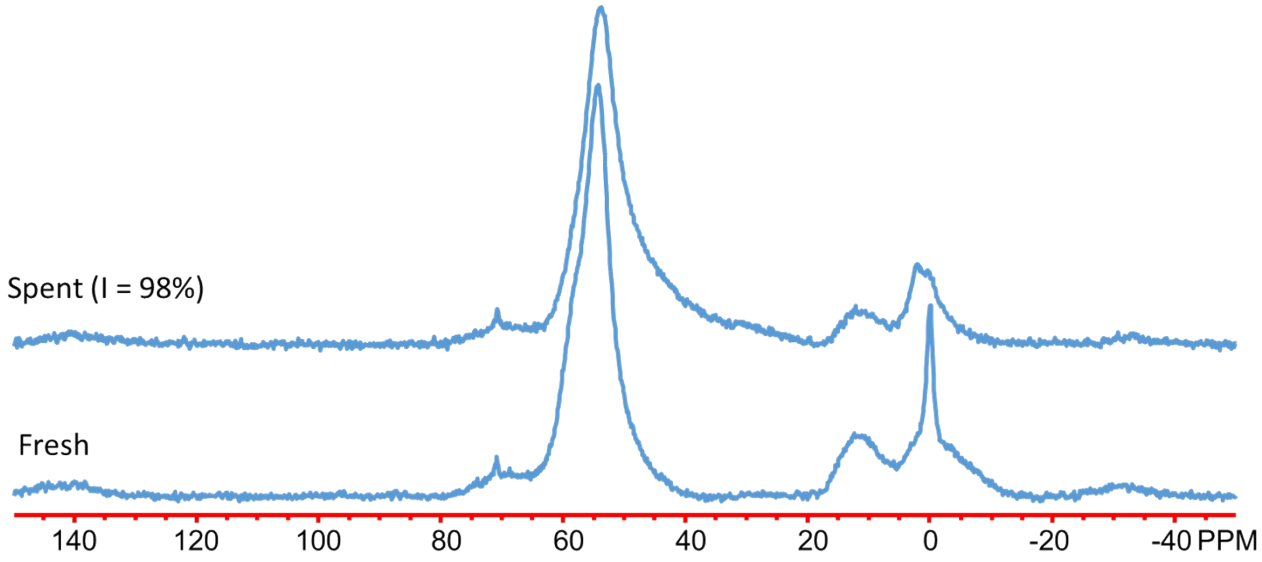

Figure S19. ^{27}Al MAS Solid-state NMR spectra for 0.4% Ni/BEA fresh (before catalysis) and spent (after C_2H_4 catalytic reaction at 220°C for 1 hour).

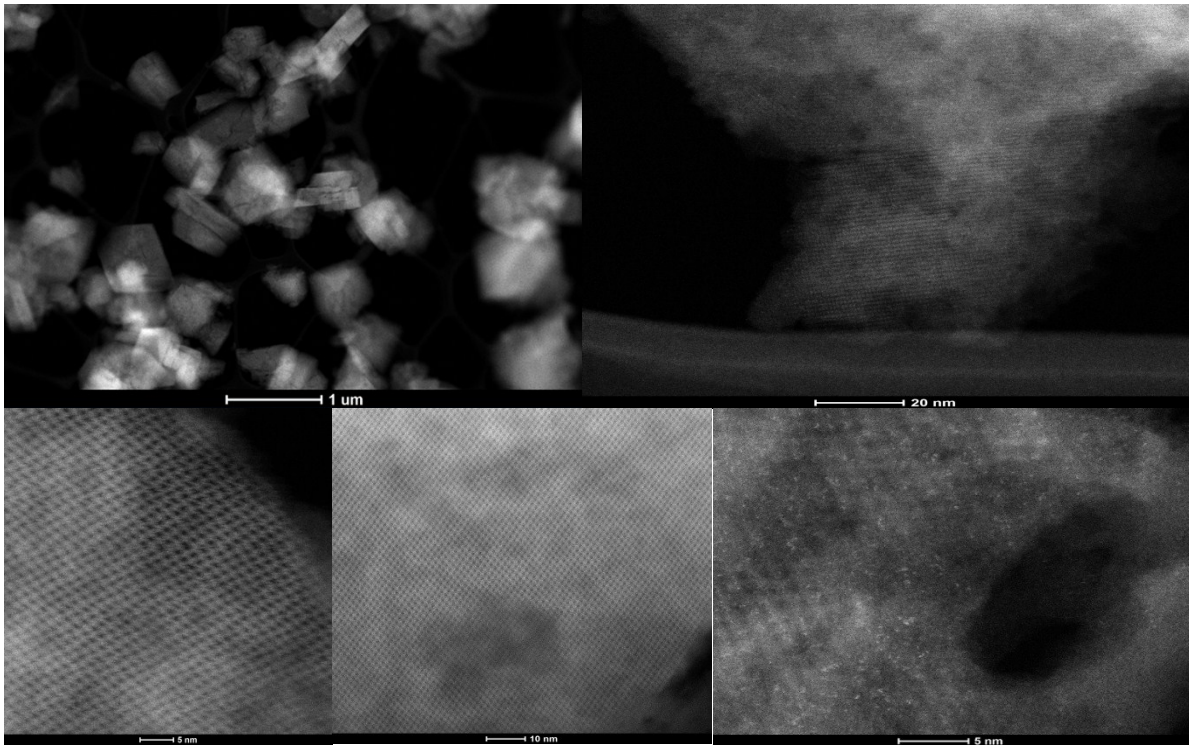

Figure S20. Additional HAADF-STEM images of 0.7% $Ir(CO)_2$/FAU in low magnification (showing absence of Ir nanoparticles) and high-magnification (showing presence of well-dispersed Ir atoms).

Table S 2. Initial TOF (with respect to butadiene formation) and selectivity to butadiene for 0.7% $Ir(CO)_2$/FAU Conditions: 30 mg, C_2H_4 flow rate 10 sccm/min, GHSV ~ 40,000 hr^{-1}

Temperature, ºC	Initial TOF, hr^{-1}	Initial Selectivity, %
80	0	0 (100% selective to butenes, TOF ~1.5 hr^{-1})
180	0	0 (100% selective to butenes, TOF ~ 20 hr^{-1})
225	203	29
250	180	31

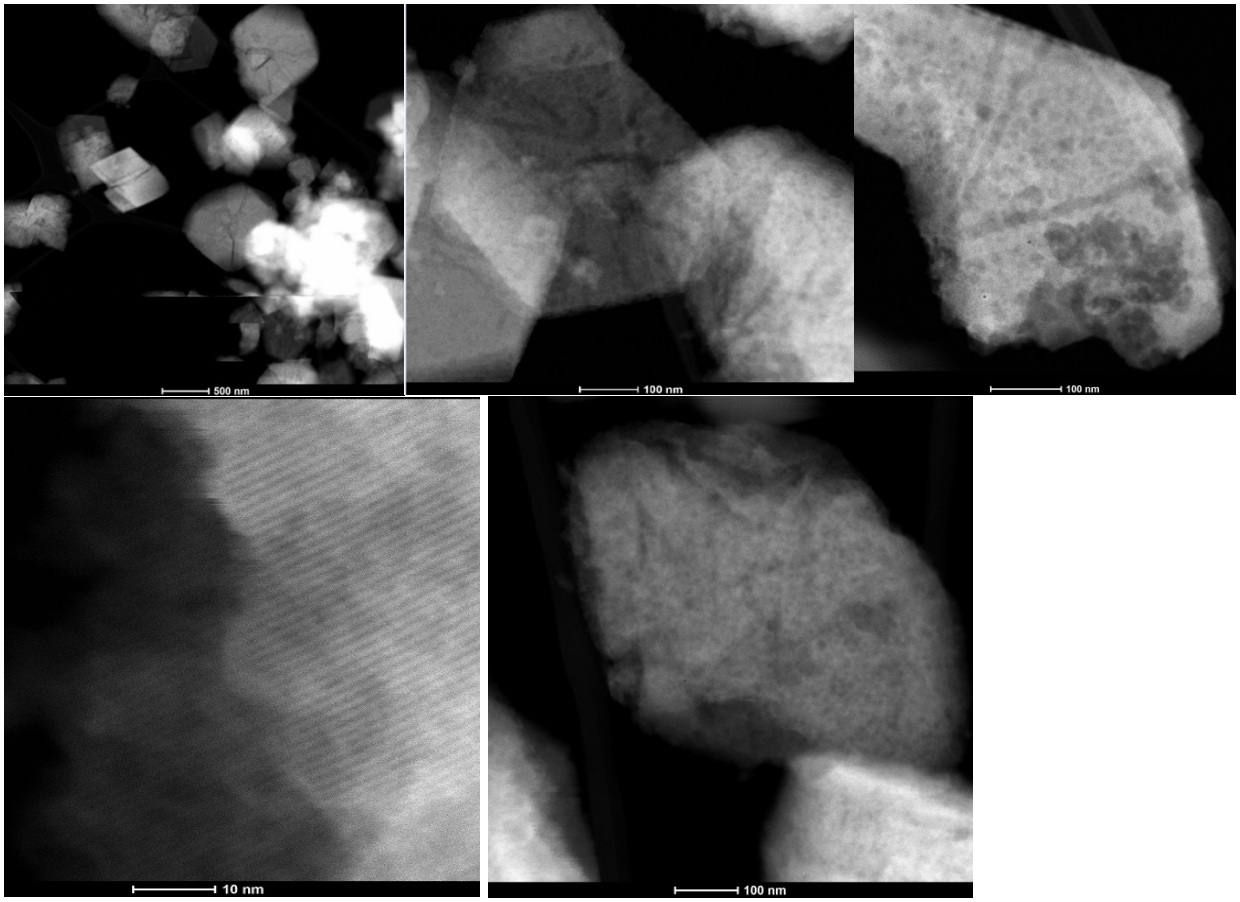

Figure S21. Additional HAADF-STEM images of 0.7% $Ir(CO)_2$/FAU, in low magnification and high-magnification after C_2H_4 catalysis at 200ºC. The sample was transferred from the reactor into the HAADF-STEM in a special sample holder void of oxygen and moisture.

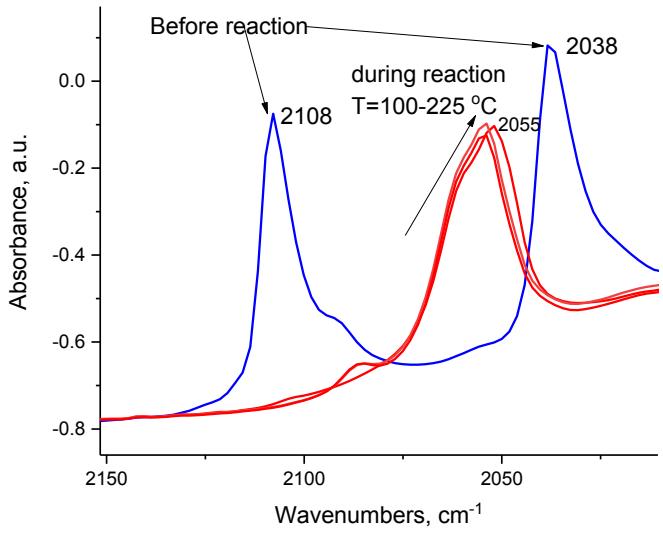

Figure S22. DRIFTS during $Ir(CO)_2$ reaction under pure C_2H_4 flow at 80-220ºC. $Ir(CO)(C_2H_4)$ is the only stable complex observed under these conditions.

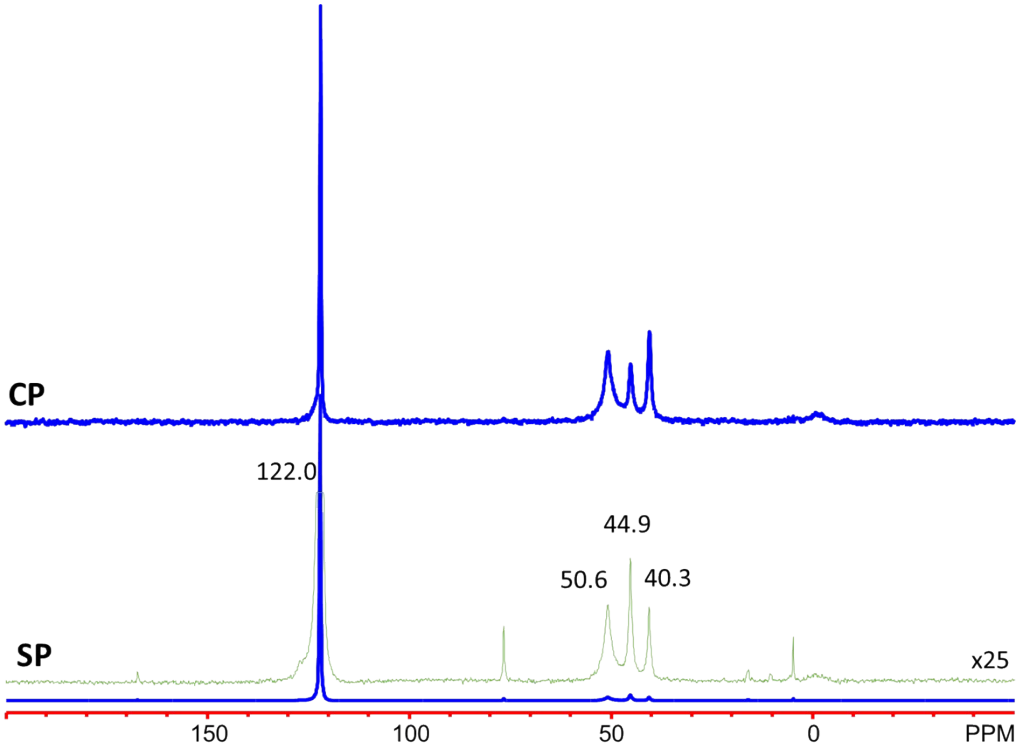

Figure S23. ^{13}C and ^{1}H-^{13}C CP MAS NMR spectra of 0.7% $Ir(CO)_2$/FAU after exposure of ~2" Hg $^{13}C_2H_4$ at room temperature. The MAS speed was 3,418 Hz. Peaks are assigned to ethylene (122 ppm, SSB: 167, 76.3 ppm), π -coordinated ethylene ligands (50.6 ppm, [J. Phys. Chem. B 2005, 109, 51, 24236-24243], and vinyl [Bulletin of the Academy of Sciences of the USSR, Division of chemical science, 1981, Volume 30, Issue 8, pp 1581, 13C NMR spectra and structure of iron carbonyl π complexes of vinylsilanes] (44.9 and 40.3 ppm), further supporting the infrared spectroscopy results. CP refers to cross-polarization. SP referese to single pulse.

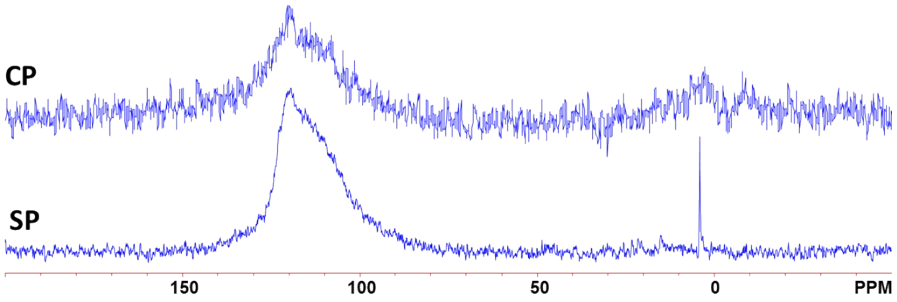

Figure S24. ^{13}C MAS Solid-state NMR spectra for 0.7% $Ir(CO)_2$/H-FAU after in situ reaction with $^{13}C_2H_4$ at 150ºC for 1 hr. Polymeric carbonaceous deposits are observed as a broad band in Cross-Polarization spectra between 80 and 150 ppm. Gas phase ethane is also present (4 ppm). [App. Cat. 1988, 45, 345-356] CP refers to cross-polarization. SP referese to single pulse.

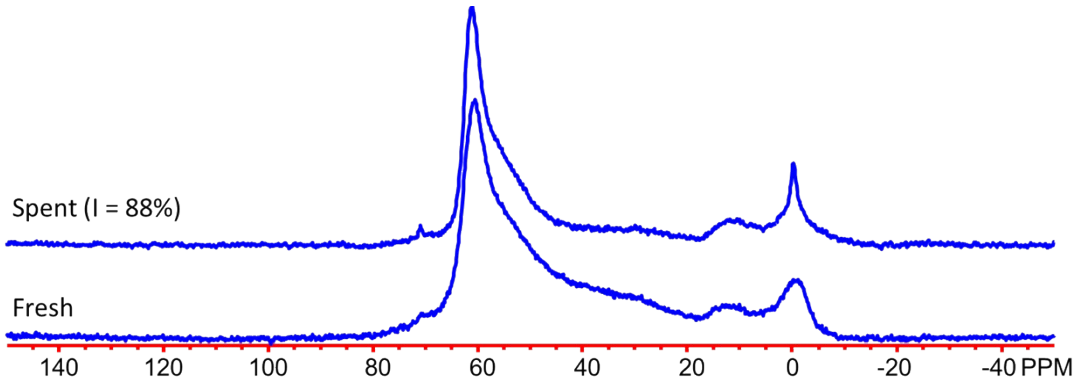

Figure S25. ^{27}Al MAS Solid-state NMR spectra for 0.7% $Ir(CO)_2$/FAU with Si/Al~15 fresh (before catalysis) and spent (after C_2H_4 catalytic reaction at 225℃ for 1 hour).

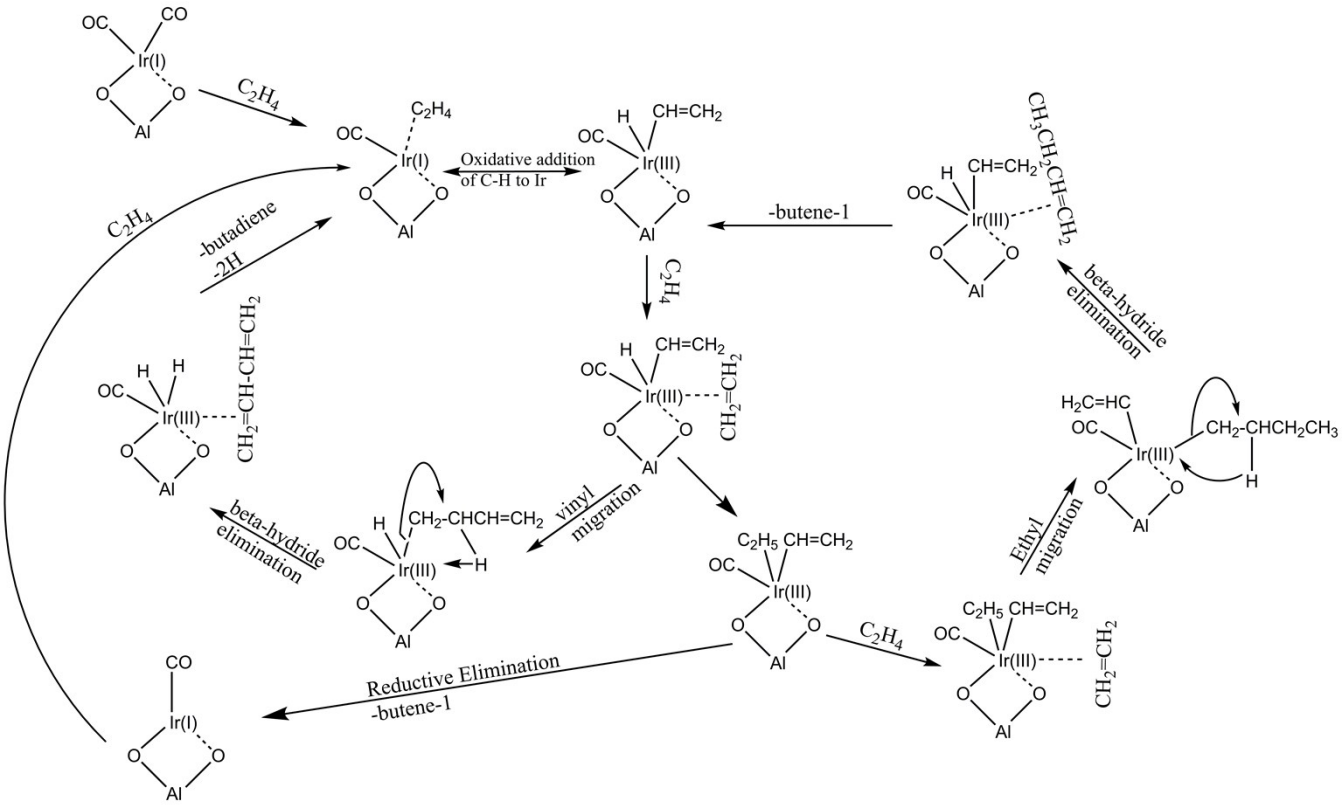

Figure S26. Probable mechanism for butene and butadiene formation from ethylene on $Ir(CO)_2$/FAU and Ni/BEA. In this mechanism C-H bond of ethylene is activated homolytically. Note, that completely analogous steps apply for Ni(II)/BEA system, except in that case no CO molecule is adsorbed on Ni. Oxidative addition of C-H bond of ethylene to Ni(II) produces Ni(IV)(H)(C_2H_3) nickel (IV) vinyl hydride species. Coordination of the metal atom to the zeolite framework is shown only as a representation and could be flexible.

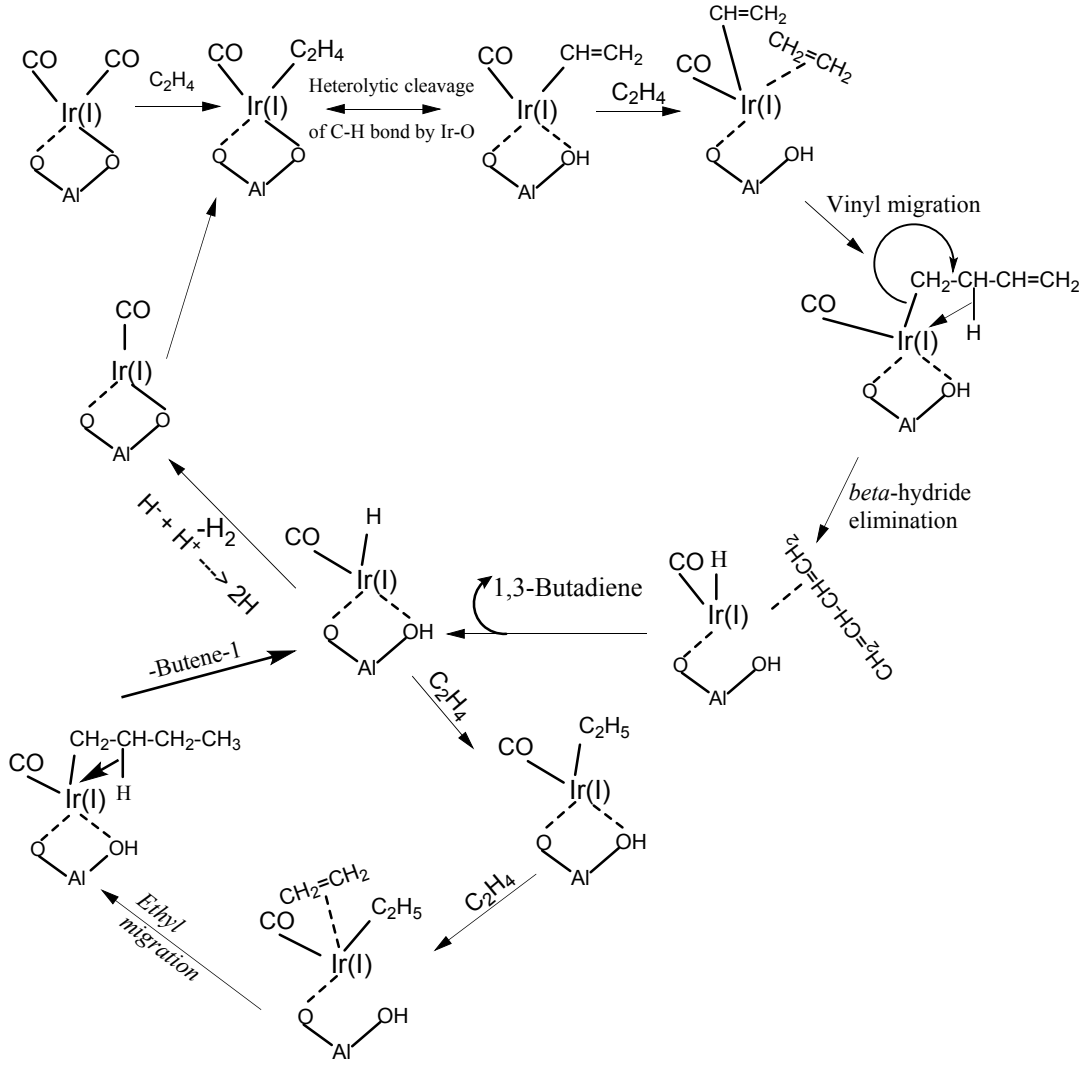

Figure S27. Probable mechanism for butene and butadiene formation from ethylene on $Ir(CO)_2$/FAU and Ni/BEA. In this mechanism, C-H bond of ethylene is activated heterolytically on Ir(I)-O and Ni(II)-O bonds. Note, that completely analogous steps apply for Ni(II)/BEA system, except in that case no CO molecule is adsorbed on Ni. Coordination of the metal atom to the zeolite framework is shown only as a representation and could be flexible.

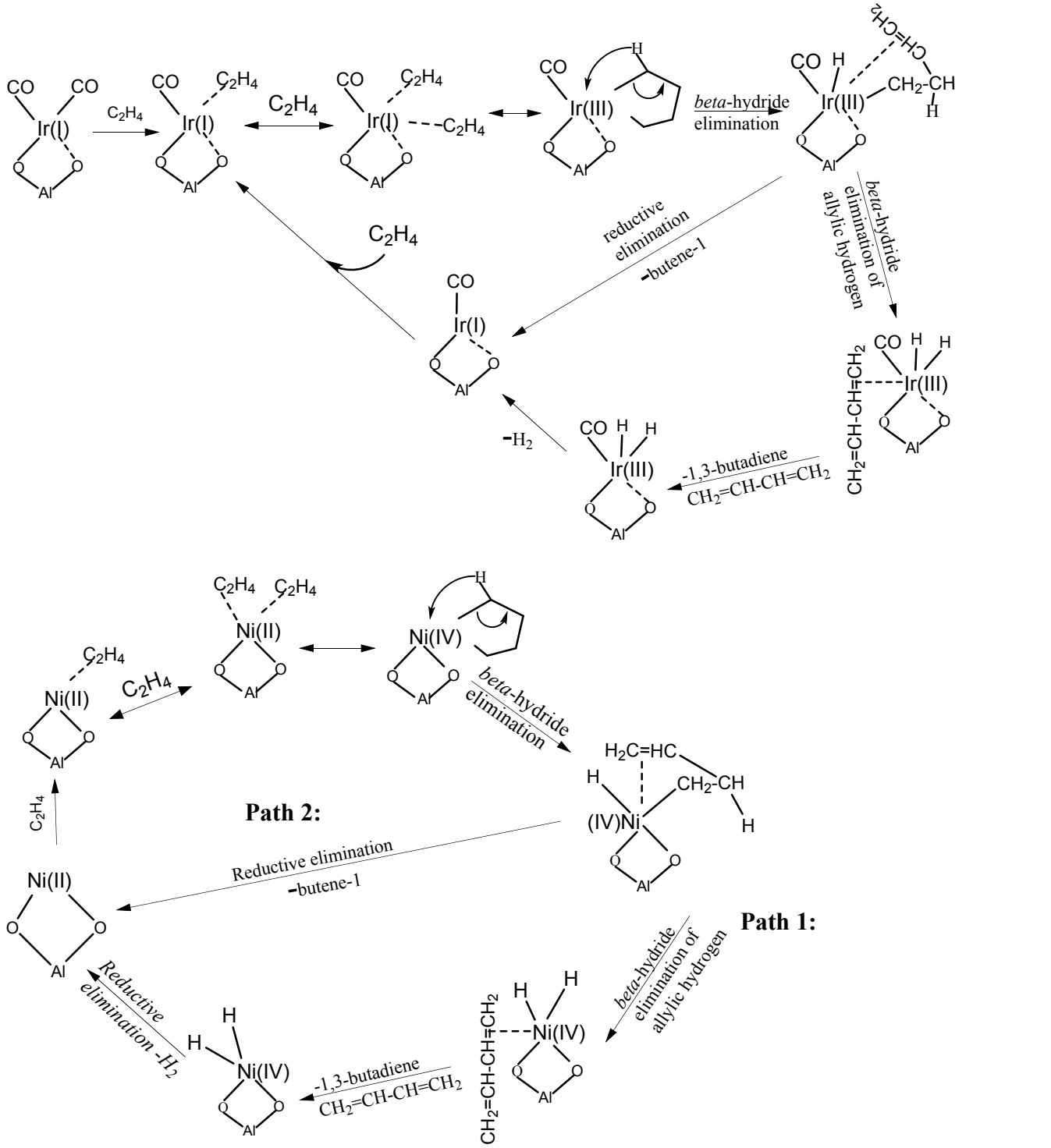

Figure S28. Mechanism for butene and butadiene formation from ethylene on $Ir(CO)_2$/H-FAU and Ni/BEA viametallocyclopentane intermediates. In this mechanism, two ethylene molecules couple on Ir(I) and Ni(II) sites with the formation or Ir(III) iridacyclopentane and Ni(IV) nickelcyclopentane intermediates initially. In the case of Ni, no CO molecules are coordinated to Ni(II). Coordination of the metal atom to the zeolite framework is shown only as a representation and could be flexible.

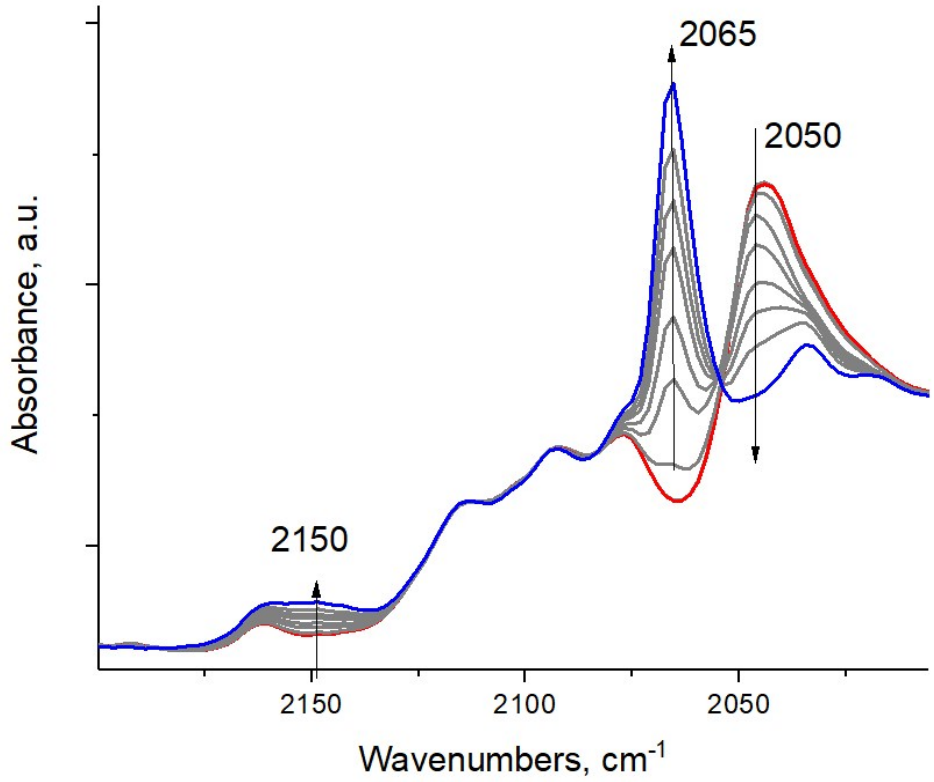

Figure S29. DRIFTS over time (1-5 minutes) of $Ir(CO)(C_2D_4)$ during reaction with pure H_2 (H_2 flow ~10 cc/min). CO band of $Ir(CO)(C_2D_4)$ at ~2,050 cm^{-1} selectively goes down and a new CO band grows at 2,065 cm^{-1}. Simultaneously, a weak band develops at 2,150 cm^{-1}, assigned to Ir-H stretch. The selective formation of $Ir(III)(CO)H_2$ complex takes place: $Ir(I)(CO)(C_2H_4) + 2\ H_2 \rightarrow Ir(III)(CO)(H)_2 + C_2H_6$

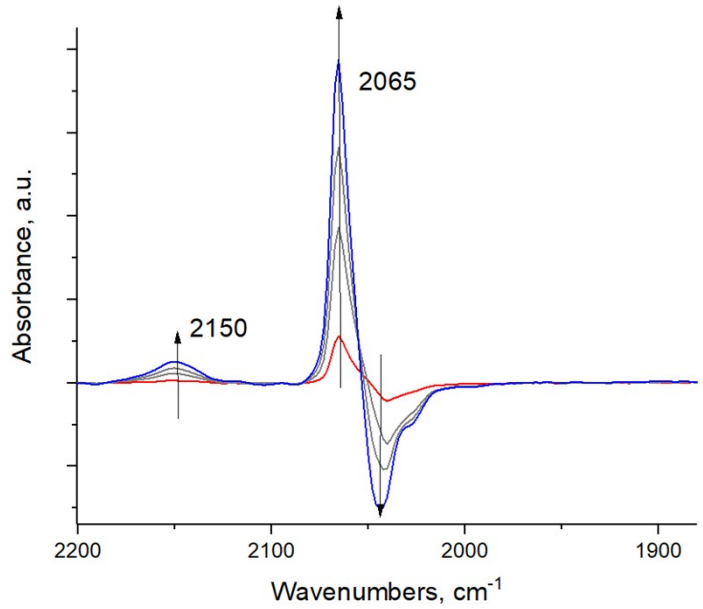

Figure S30. DRIFTS difference spectra (in time 1-5 minutes) during $Ir(CO)(C_2D_4)$ during reaction with pure H_2 (H_2 flow ~10 cc/min). This shows clean selective conversion of $Ir(I)(CO)(C_2D_4)$ to $Ir(III)(CO)(H)_2$. Unlike Rh(III)(CO)(H)x/FAU which has a complex Rh-H band structure due to the formation of families of rhodium carbonyl hydride complexes with undissociated and dissociated hydrogen ligands $Rh(I)(CO)(H_2)$ and $Rh(III)(CO)(H)_2$ in FAU micropores (see references 17 and 18 in the main text), the Ir sample shows clean conversion to $Ir(III)(CO)(H)_2$

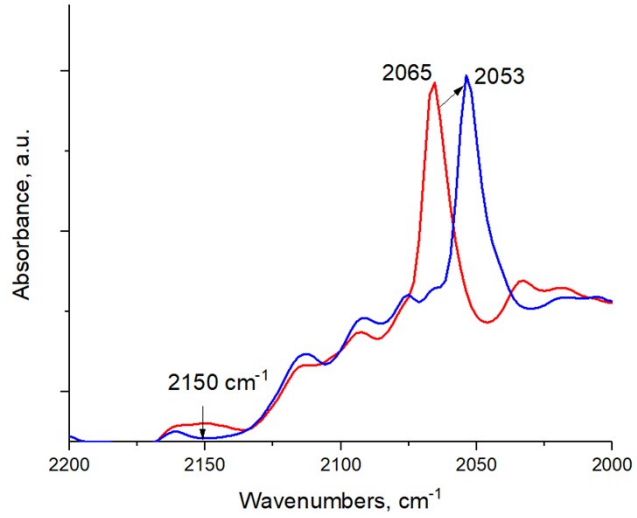

Figure S31. DRIFTS in time (2 minutes) during $Ir(III)(CO)H_2$ reaction with D_2. The following reaction takes place: $Ir(III)(CO)(H)_2 + D_2 \rightarrow Ir(III)(CO)(D)_2 + H_2$; this fully confirms our assignment of 2150 cm^{-1} band to the Ir-H stretch, it disappears due to the formation of the Ir-D bond.

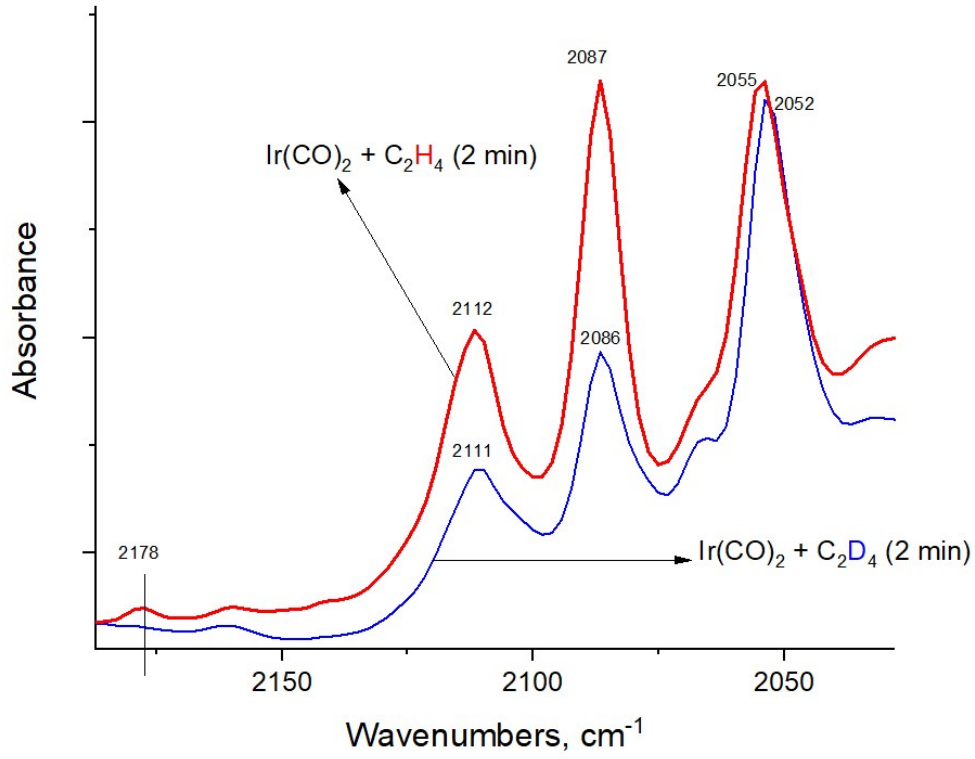

Figure S32. Comparison of DRIFTS spectra after the first 2 minutes of [$Ir(CO)_2$/FAU+C_2H_4] reaction (red spectrum) and [$Ir(CO)_2$/FAU + C_2D_4] reaction (blue spectrum). Note, that the 2,178 cm^{-1} Ir-H band is absent in the C_2D_4 treated spectrum, confirming it is not a CO vibration but Ir-H vibration.

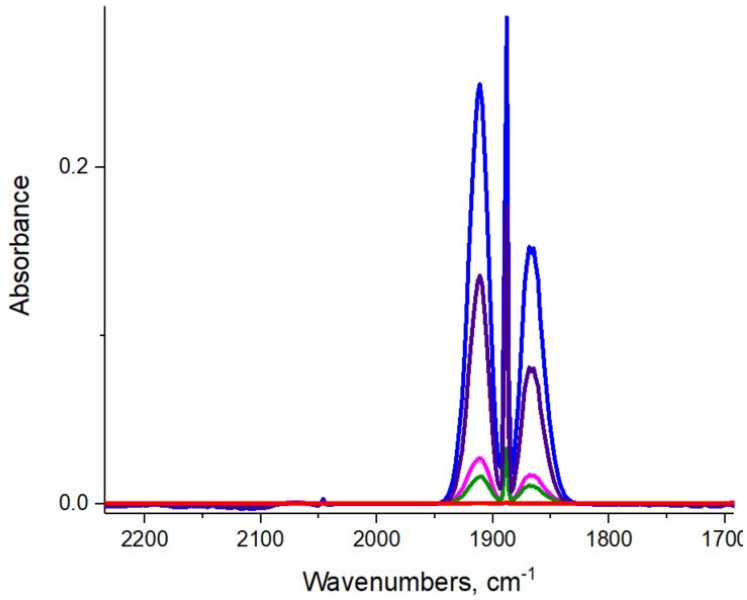

Figure S33. DRIFTS spectra during ethylene interaction Ni/BEA, showing no discernible features that could be attributed to Ni-H species. Dehydrated Ni/BEA sample was used as a background. Ethylene was flowed through the cell (blue spectrum in ethylene flow), we then purged ethylene with He continuously. The isoelectronic nature of Ni(IV), Rh(III), and Ir(III) hydrides, it is expected that the Ni(IV)-H stretch arise in the 2,100 cm^{-1} region. We note, however, that we were unable to observe the Ni(IV)-H intermediates either due to their small abundance and/or metastable nature. Furthermore, we believe that the Ni(IV)-H band stretching IR frequency would be difficult to identify is due to the low molar extinction coefficients of such species. Few such Ni-H IR frequencies are reported for well-defined organometallic nickel (I and II) hydride complexes for the same reason, and no to our knowledge no Ni(IV)-H complex has ever been reported. Only recently has Melanie Sanford's group produced and characterized these extremely metastable Ni(IV) complexes crystallographically under special conditions and with specialized ligands. More work is underway in our laboratory to identify the elusive intermediates for Ni/Zeolite system.